Oncogene (2010) 29, 2973–2982

www.nature.com/onc

ORIGINAL ARTICLE

Human TRIB2 is a repressor of FOXO that contributes to the malignant phenotype of melanoma cells

F Zanella[1], O Renner[1], B García[1], S Callejas[2], A Dopazo[2], S Peregrina[1], A Carnero[1] and W Link[1]

[1]*Experimental Therapeutics Program, Centro Nacional de Investigaciones Oncologicas (CNIO), Madrid, Spain and* [2]*Genomics Unit, Centro Nacional de Investigaciones Cardiovasculares (CNIC), Madrid, Spain*

FOXO transcription factors are evolutionarily conserved proteins that orchestrate gene expression programs known to control a variety of cellular processes such as cell cycle, apoptosis, DNA repair and protection from oxidative stress. As the abrogation of FOXO function is a key feature of many tumor cells, regulation of FOXO factors is receiving increasing attention in cancer research. In order to discover genes involved in the regulation of FOXO activity, we performed a large-scale RNA-mediated interference (RNAi) screen using cell-based reporter systems that monitor transcriptional activity and subcellular localization of FOXO. We identified genes previously implicated in phosphoinositide 3-kinase/Akt signaling events, which are known to be important for FOXO function. In addition, we discovered a previously unrecognized FOXO-repressor function of *TRIB2*, the mammalian homolog of the *Drosophila* gene *tribbles*. A cancer-profiling array revealed specific overexpression of *TRIB2* in malignant melanoma, but not in other types of skin cancer. We provide experimental evidence that *TRIB2* transcript levels correlate with the degree of cytoplasmic localization of FOXO3a. Moreover, we show that *TRIB2* is important in the maintenance of the oncogenic properties of melanoma cells, as its silencing reduces cell proliferation, colony formation and wound healing. Tumor growth was also substantially reduced upon RNAi-mediated TRIB2 knockdown in an *in vivo* melanoma xenograft model. Our studies suggest that TRIB2 provides the melanoma cells with growth and survival advantages through the abrogation of FOXO function. Altogether, our results show the potential of large-scale cell-based RNAi screens to identify promising diagnostic markers and therapeutic targets.
Oncogene (2010) **29,** 2973–2982; doi:10.1038/onc.2010.58; published online 8 March 2010

Keywords: TRIB2; FOXO; melanoma; RNAi; screening

Correspondence: Dr W Link, Experimental Therapeutics, Centro Nacional de Investigaciones Oncologicas (CNIO), Melchor Fernandez Almagro, 3, Madrid 28029, Spain.
E-mail: wlink@cnio.es
Received 28 October 2009; revised 7 January 2010; accepted 13 January 2010; published online 8 March 2010

Introduction

FOXO transcription factors are *bona fide* tumor suppressors that are inactivated in the majority of human cancers, owing to the overactivation of the phosphoinositide 3-kinase (PI3K)/Akt pathway (Dansen and Burgering, 2008). The four members of the mammalian FOXO family of proteins—FOXO1, FOXO3a, FOXO4 and FOXO6—belong to class O of the forkhead/winged helix transcription factors (Fox). FOXO proteins can regulate a variety of genes that influence cell proliferation, survival, metabolism and response to stress (Huang and Tindall, 2007). The FOXOs are regulated by synthesis, phosphorylation, acetylation and ubiquitination at three different levels: subcellular localization, stability and transcriptional activity (Myatt and Lam, 2007). Upon the activation of PI3K/Akt signaling, FOXOs undergo Akt-mediated phosphorylation, which promotes binding to 14-3-3, nuclear export through CRM1 and cytoplasmic sequestration. Under stress conditions or in the absence of growth or survival factors, when the PI3K/Akt pathway is inhibited, FOXO proteins translocate to the cell nucleus, where their transcriptional functions can be executed (Brunet *et al*., 1999).

Triple knockout mouse models proved the tumor suppressor properties of FOXOs, as mice simultaneously lacking the principal members of the mammalian FoxO subfamily, FoxO1, FoxO3a and FoxO4, are prone to develop hemangiomas and lymphoproliferative diseases (Paik *et al*., 2007). Conversely, the individual or paired inactivation of FoxO1, FoxO3a or FoxO4 resulted in a less severe phenotype, supporting the idea of functional redundancy of these FOXO factors (Paik *et al*., 2007). Furthermore, forced expression of FOXO has been shown to curb tumorigenesis in xenograft experiments using human tumor cell lines grown in nude mice (Hu *et al*., 2004; Yang *et al*., 2005). Therefore, reactivation of FOXO based on its tumor suppressor properties is considered as a very attractive anti-cancer strategy. Contrary to other tumor suppressors such as p53 or PTEN, the functions of which are abrogated by genetic or epigenetic changes, inactivation of FOXOs occurs mostly because of the overactivation of their inhibitory inputs (Dansen and Burgering, 2008). This offers a wide range of possibilities for restoring FOXO activity with small-molecule inhibitors targeting up-regulated FOXO repressors. Nevertheless, as FOXO

also induces genes involved in resistance to cellular stress, including the multi-drug resistance gene *ABCB1* (Gomes *et al*., 2008; Hui *et al*., 2008), such a strategy has to be carefully evaluated and the most suitable points of intervention must be identified. The transcriptional program finally executed by FOXO is thought to be dependent on the pattern of its post-transcriptional modifications (Calnan and Brunet, 2008). Hence, characterization of the components that participate in the signaling network that controls the activity of FOXO is essential to reveal possible therapeutic targets for future anticancer therapies. To identify endogenous suppressors of FOXO, which could be exploited pharmacologically to restore FOXO function in human tumors, we conducted a systematic large-scale loss-of-function screening. Among the genes identified and validated as negative FOXO regulators, we found the pseudokinase *TRIB2*. *In vitro* and *in vivo* results reported here indicate that *TRIB*2 can facilitate the growth and survival of melanomas by downregulating FOXO activity.

Results

Generation of the 293foxREP cell line

To establish a cell line capable of measuring the transcriptional activity of FOXO and suitable for a transfection-based RNA-mediated interference (RNAi) screening, we introduced the reporter construct pGLpuro-3xDBE (Zanella *et al*., 2009) into human embryonic kidney (HEK)293T cells. pGLpuro-3xDBE contains three copies of the DBE consensus cassette in front of an SV40 minimal viral promoter linked to a firefly luciferase reporter gene and a puromycin-resistance cassette (Supplementary Figure S1A). Stable 293foxREP cells showed a strong responsiveness to inhibition of the PI3K/Akt pathway (Supplementary Figure S1B) and hence proved to be suitable tools to screen for the interference with FOXO regulation.

Screening of an RNAi library against 7914 human genes

The identification of all components involved in the regulatory network that determines the activity of FOXO proteins is an essential step to develop targeted therapies that reactivate specific FOXO functions in human tumors. Hence, we performed a large-scale loss-of-function screen aimed at the identification of genes that suppress the transcriptional activity and nuclear localization of FOXO transcription factors (Supplementary Figure S2). We used a vector-based RNAi library against 7914 human genes, each of them targeted by a pool of three different short hairpin RNA (shRNA), which has been widely used for target discovery efforts (Berns *et al*., 2004). We cotransfected each shRNA pool along with a constitutive expression vector containing the FOXO gene and another containing the *Renilla* luciferase gene into 293foxREP cells and monitored the firefly luciferase activity normalized against *Renilla* luciferase. Those shRNAs pools that generated a normalized luciferase activity greater than threefold the activity of the control shRNA vector were analyzed for its capacity to induce nuclear translocation of FOXO in the U2foxRELOC system that has been described previously (Zanella *et al*., 2008). Briefly, U2foxRELOC cells stably express a green fluorescent protein-tagged version of FOXO3a to monitor the subcellular localization of FOXO proteins. We prioritized those hits scoring positive in both 293foxREP and U2foxRELOC cells (Supplementary Table S1). Among these dual hits were several genes known to be part of the PI3K/Akt network, including PIK3CA and Akt-3, indicating the specificity of our screening strategy. Importantly, several genes previously not associated with the regulation of FOXO activity were identified.

Validation of TRIB2 silencing

The RNAi-mediated silencing of *TRIB2*, the human homolog of the *Drosophila* gene *tribbles*, resulted in the induction of FOXO-dependent transcription in 293foxREP cells and the nuclear translocation of FOXO3a in U2foxRELOC cells. We isolated and verified the sequences of the three components of the corresponding shRNA pool. Quantitative PCR analysis revealed that two of the three shRNAs of the pool were capable of silencing TRIB2 transcript levels. To validate our findings using independent RNAi agents against TRIB2, we analyzed several siRNA oligonucleotides as well as vector-based shRNA constructs for their silencing efficiency against TRIB2. These shRNAs and siRNAs were chosen to contain different 5′-portions of the guide strand that has been implicated in unintended transcript silencing (Birmingham *et al*., 2006). Several RNAi-based agents effectively reduced the expression of TRIB2 (Supplementary Table S2). Two different vector-based shRNA constructs—TRIB2^{NKI} shRNA and TRIB2^{ORI} shRNA—proved to be the most efficient tools to silence TRIB2 and were used for further analysis. Figure 1a shows the reduction of TRIB2 mRNA upon the transfection of HEK293T cells with TRIB2^{NKI} shRNA as compared with cells transfected with the corresponding control vector. Importantly, transient expression of the TRIB2^{NKI} shRNA resulted in increased FOXO-driven luciferase activity (Figure 1b) and nuclear localization of GFP–FOXO (Figures 1c and d). In contrast, unrelated shRNA sequences failed to produce similar effects on FOXO (data not shown). On the other hand, the overexpression of a V5-tagged version of TRIB2, which was detected by western blot analysis using a V5-specific antibody (Figure 2a), markedly decreased FOXO-driven luciferase activity in 293foxREP cells (Figure 2b). Silencing or overexpression of TRIB2 produced very similar effects on FOXO family member FOXO1 (data not shown). These results suggest that TRIB2 acts as a FOXO repressor, promoting its cytoplasmic sequestration and impairing its transcriptional control function.

TRIB2 transcript levels are elevated in malignant melanoma

The implication of TRIB2 in the regulation of the tumor suppressor FOXO prompted us to analyze its expression levels in human tumors. To that end, we used a cancer

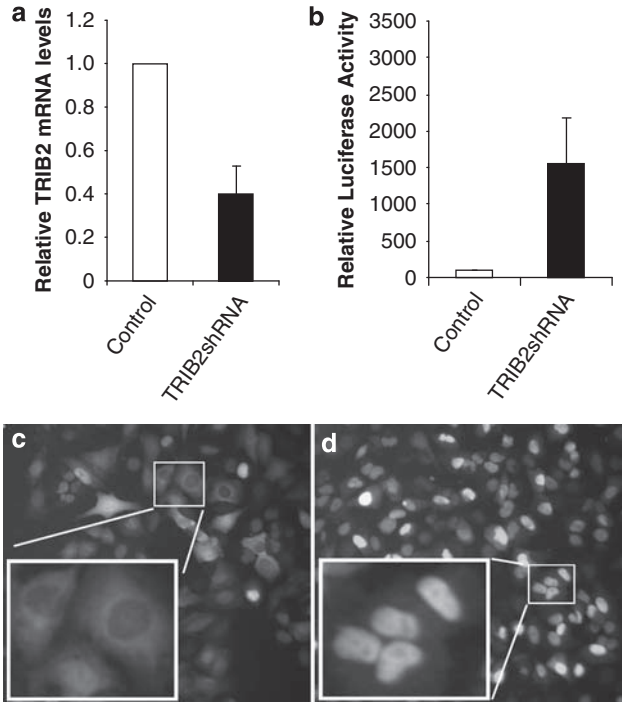

Figure 1 Silencing of TRIB2 induces FOXO-driven luciferase activity and nuclear translocation of GFP–FOXO. (**a**) Relative TRIB2/GAPDH mRNA levels after transfection of HEK293T cells with the shRNA construct TRIB2_NKI. Cells were harvested 48 h after transfection and processed for quantitative PCR using the methods described above. (**b**) Transcriptional activity of FOXO upon silencing of TRIB2 with the shRNA construct TRIB2_NKI as measured by FOXO-driven expression of luciferase in co-transfection experiments. Each construct was transiently co-transfected with plasmids encoding FOXO3a and *Renilla* luciferase into 293foxREP cells, and the luciferase activities were determined as described in Materials and methods. The data were normalized to the *Renilla* luciferase (phRG-TK vector) reporter construct. The results are given as the mean ± s.e.m. of three independent experiments performed in triplicate. (**c, d**) Subcellular localization of fluorescent FOXO reporter protein after transfection of U2foxRELOC cells with control vector (**c**) or shRNA construct TRIB2_NKI (**d**).

profiling array containing samples from 154 patients with different tumors, including the breast, ovary, colon, stomach, lung, kidney, bladder, vulva, prostate, uterus, cervix, rectum, thyroid, testis, skin, small intestine and pancreas. For this array, complementary DNAs (cDNA) generated from matched normal and tumor tissue samples from individual patients had been spotted side by side on a nylon membrane. In addition, cDNAs from nine different cancer cell lines have been included (Supplementary Figure S3). Interestingly, elevated levels of TRIB2 mRNA were observed in 7 out of 10 skin cancer samples (Figures 3a and b). Moreover, the seven samples that showed high TRIB2 expression correspond to malignant melanoma lesions (Figure 3a: P1–P5, P9, P10), whereas the remaining three samples (Figure 3a: P6, P7 and P8) that did not show a significant increase of TRIB2 transcripts refer to squamous-cell carcinomas (Supplementary Table S3). Consistently, we detected the highest level of TRIB2 transcripts in G-361 melanoma cells when compared with eight other non-melanoma cells represented on the same membrane (Figures 3c and d). To confirm this observation, we analyzed an independent arrayed panel of 43 pre-normalized cDNAs selected from normal and melanoma tissues and from mixed ages and genders (Supplementary Table S4). qRT–PCR analysis of these samples revealed a significantly increased level of TRIB2 expression in malignant melanoma diagnosed at stage III or IV when compared with normal skin tissues (Supplementary Figure S2C). The same pattern was reproduced when the mRNA level of TRIB2 was analyzed in a panel of melanoma cell lines versus non-melanoma cell lines by qRT–PCR. We detected an abundance of TRIB2 transcripts between 3 and 23 times greater in cell lines derived from melanoma biopsies than in non-melanoma cells including keratinocytes and fibroblasts (Figure 4a). Interestingly, human epidermal melanocytes also showed high levels of TRIB2 transcripts. The levels of Bim, a pro-apoptotic molecule transcriptionally regulated by FOXO, were also assessed. We observed an inverse correlation between the transcript levels of TRIB2 and Bim (Figure 4b). In human epidermal melanocytes and melanoma cells, high expression of TRIB2 coincides with very low levels of Bim transcripts. In contrast, non-melanoma cell lines with low level of TRIB2 transcription showed increased abundance of Bim transcripts. Accordingly, the levels of TRIB2 expression correlate with the subcellular localization of fluorescently labeled FOXO reporter protein, which we introduced stably into melanoma and non-melanoma cell lines (Figure 4c). Taken together, these data suggest that overexpression of TRIB2 leads to the reduction of FOXO activity in melanocyte-derived cells.

TRIB2 knockdown increases the activity of FOXO in melanoma

To assess the influence of TRIB2 on FOXO functions in melanoma, G-361 human melanoma cells were adopted as a model, as they show increased levels of TRIB2 mRNA (see above). G-361 cells stably expressing a GFP–FOXO3a fusion protein and the FOXO-driven luciferase reporter construct pGL3puro-3xDBE, hereafter designated as G-361FireFox, were transiently transfected with shRNA agents against TRIB2, PIK3-CA, Akt or their respective empty control plasmids. A significant increase in luciferase-produced luminescence was detected upon silencing of TRIB2, coincident with the nuclear relocalization of the GFP–FOXO fusion protein. The effect obtained was comparable to FOXO stimulation via the knockdown of PI3K or Akt (Supplementary Figure S4). In contrast, unrelated shRNA sequences failed to produce similar effects on FOXO (data not shown). These data support the hypothesis that TRIB2 may function as a FOXO repressor and prove this G-361FireFox model to be suitable to analyze the role of TRIB2 in malignant melanoma.

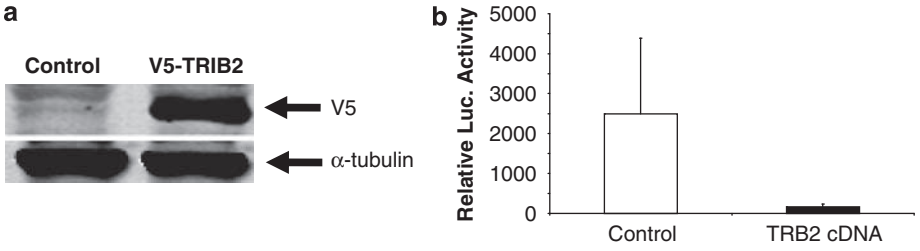

Figure 2 Ectopic expression of TRIB2 reduced FOXO-driven luciferase expression. (**a**) TRIB2 cDNA was tagged with a V5 epitope and expressed in HEK293T cells. Overexpression was detected by western blot analysis using a specific antibody against the V5 tag. Equal loading was confirmed by the specific detection of α-tubulin expression. Relevant proteins are indicated by arrows in the blot from a representative experiment. (**b**) Luciferase expression from a FOXO-driven promoter was monitored upon expression of control plasmid or V5-tagged TRIB2 cDNA. Each construct was transiently co-transfected with plasmids encoding FOXO3a and *Renilla* luciferase into 293foxREP cells, and the luciferase activities were determined as described above. The data were normalized to the Renilla luciferase (phRG-TK vector) reporter construct. The results are given as the mean ± s.e.m. of three independent experiments performed in triplicate.

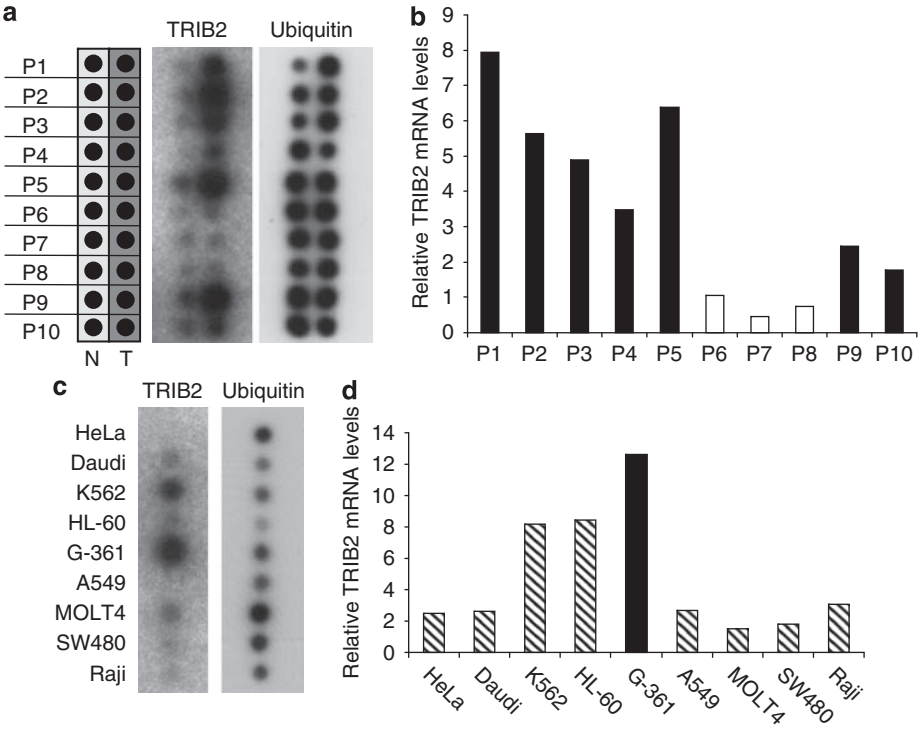

Figure 3 TRIB2 is overexpressed in malignant melanoma. A cancer-profiling array was hybridized separately with a radiolabeled probe for the housekeeping gene ubiquitin and a radiolabeled probe for TRIB2. Hybridization signals were detected by phosphoimaging. (**a**) Samples from 10 patients (P1–P10) with skin cancer and matched normal tissue are shown. N = normal; T = tumor. (**b**) Quantification of TRIB2 levels was performed using Quantity One software. The hybridization signals for TRIB2 were normalized against signals obtained for ubiquitin. Then, the ratio between normalized values from normal tissue to those from tumors was calculated for each patient (P1–P10). Black bars represent malignant melanoma, white bars indicate non-melanoma skin cancer. (**c**) Hybridization signals from nine different cancer cell lines were shown. (**d**) Quantification of TRIB2 levels was performed as described above. Black bars represent melanoma cells; dashed bars indicate non-melanoma cancer cell lines.

TRIB2 facilitates the growth and survival of melanoma cells

In order to investigate the importance of TRIB2 for melanoma cells, we developed a stable knockdown system for TRIB2. G-361 melanoma cells were transfected either with a control vector (361C) or with an shRNA against TRIB2 (361shTRIB). TRIB2 mRNA levels were monitored in several independent cell clones expanded from single puromycin-resistant colonies after stable transfection by qRT–PCR. Figure 5a shows that continuous silencing of TRIB2 in 361shTRIB cells led to a 10-fold decrease of TRIB2 mRNA compared with the transcript level in 361C cells.

In order to explore the role of TRIB2-mediated FOXO inactivation in melanoma, we assessed the tumorigenic properties of the melanoma knockdown system previously generated. 361C and 361shTRIB cells were seeded and maintained in standard growth factor

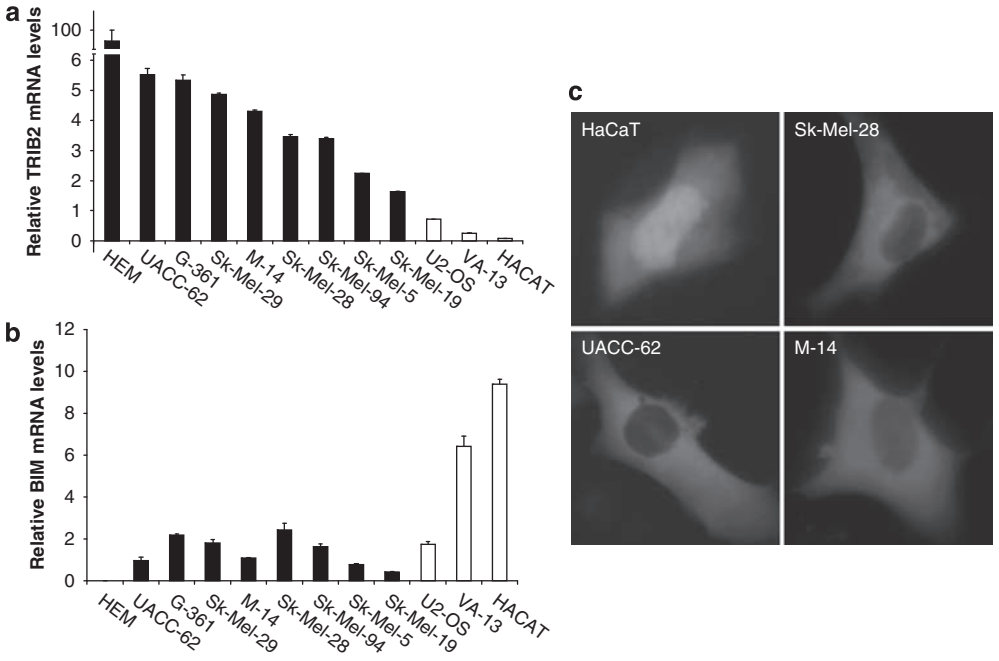

Figure 4 TRIB2 expression negatively correlates with Bim expression and nuclear FOXO localization. qRT–PCR analysis of TRIB2 (**a**) and Bim (**b**) mRNA levels in a panel of cell lines. Black bars refer to melanocyte-derived cells, while white bars correspond to non-melanocyte derived cells. Error bars refer to standard error. Normalization of the results was performed by taking 18S mRNA levels as reference. (**c**) Subcellular localization of fluorescently labeled FOXO reporter protein stably expressed in HaCaT keratinocytes and in the melanoma cell lines Sk-Mel-28, UACC-62 and M-14. Representative images are shown.

conditions, while cell growth was monitored every other day by crystal violet staining. The absorbance of the cell lysis products was taken as an indirect measurement of the cell growth. 361shTRIB cells showed a significantly decreased proliferation rate when compared with 361C cells (Figure 5b), indicating that TRIB2 expression confers growth advantage to those melanoma cells. To determine whether TRIB2 influences the ability of melanoma cells to overcome apoptosis in the absence of cell contact, 10^4 361C or 361shTRIB cells were seeded at low density and allowed to grow over a period of 10 days. Then cells were fixed, stained and the number of colonies quantified. 361C cells bypassed more efficiently the barriers of low-density seeding than 361shTRIB cells, as the latter generated a significantly reduced number of colonies in this assay (Figure 5c). These data have been confirmed for different cell clones. Furthermore, re-expression of mouse trb2, which is resistant to the stable silencing in 361shTRIB cells, was sufficient to rescue the aggressive phenotype of 361C cells, thereby unambiguously relating these observations to the silencing of TRIB2.

The ability of 361C or 361shTRIB cells to grow in anchorage-independent conditions was analyzed by seeding 10^5 cells in soft agar and allowing them to grow for 1 month. Importantly, 361C cells produced a significantly greater number of foci than 361shTRIB cells (Figure 5d). Furthermore, the foci formed by 361C cells showed increased size (Figure 5e).

To investigate the influence of TRIB2 in the migration properties of melanoma cells, both cell lines were seeded in 24-well plates and allowed to reach confluence. At that point, a wound was produced in the central vertical axis of each well and a fixed point of reference for microscopic photography was set. Pictures taken every 24 h indicated a greater efficiency of 361C cells in refilling the wounded area, closing the wound over a period of 72 h, whereas 361shTRIB cells were unable to refill the wounded area even after 96 h (Figure 5f). Furthermore, 361shTRIB cells showed contact inhibition upon reaching confluence, whereas 361C cells piled up and formed colonies beyond the cell monolayer, a feature of transformed cells (Figure 5f). Taken together, these results support the hypothesis that TRIB2 is necessary for the maintenance of the tumorigenic properties of melanoma cells.

TRIB2 knockdown impairs melanoma growth in vivo

To investigate the possible effects of TRIB2 knockdown in settings that resemble with more fidelity *in vivo* tumorigenesis, 7×10^5 361C or 361shTRIB cells, respectively, were xenografted subcutaneously in ZSCID mice, and their respective tumor growth was followed over a period of 10 weeks. Tumor development occurred significantly faster in mice injected with control cells (361C) when compared with animals in which TRIB2 knockdown cells (361shTRIB) were implanted (Figure 6a). On day 69, pictures taken from the animals before killing and after tumor resection show a clear difference in the *in vivo* growth potential of the cell populations implanted (Figure 6b). Whereas 361C cells produced larger, spherical tumors, 361shTRIB cells rarely grew beyond a few mm^3.

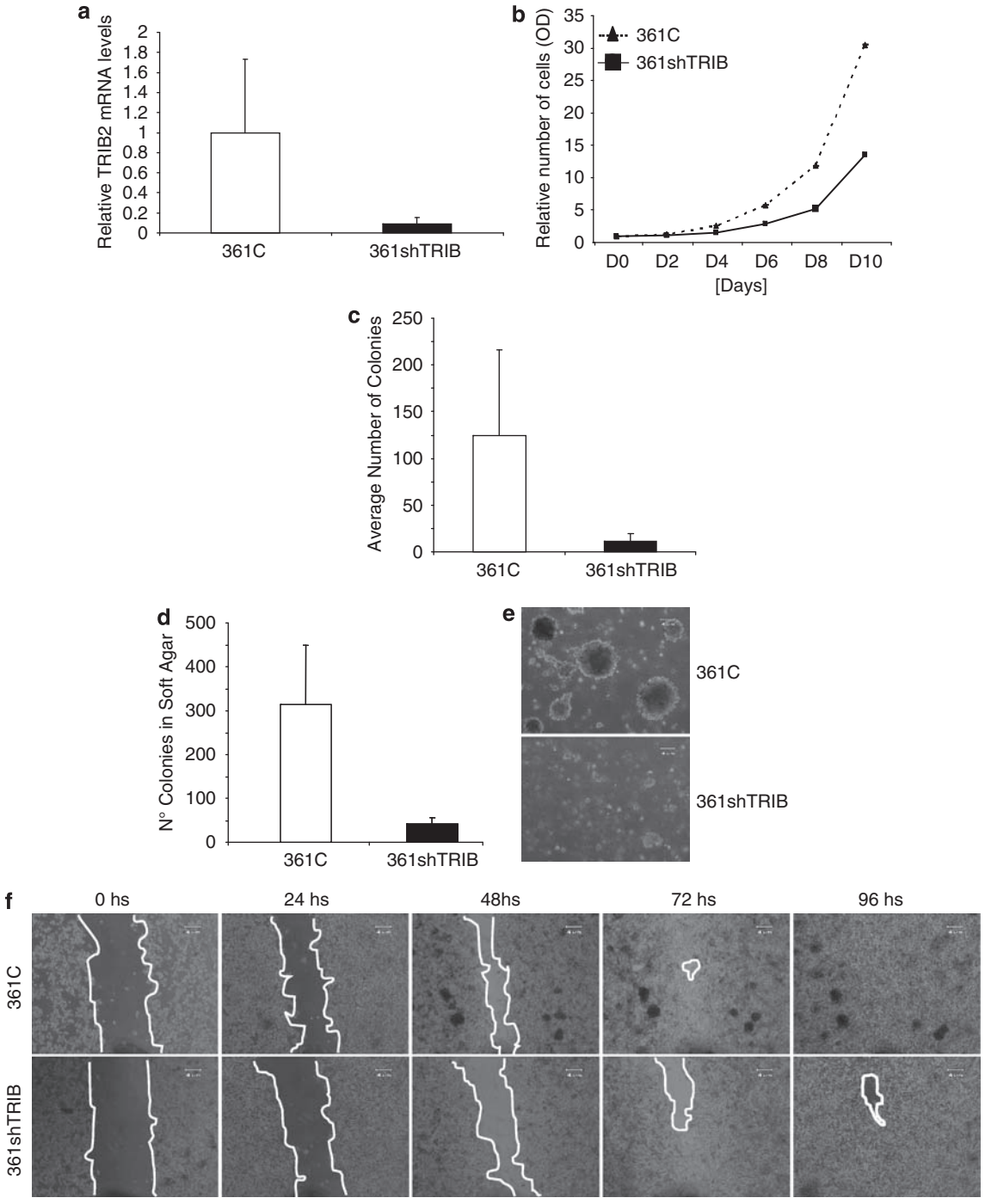

Figure 5 Silencing of TRIB2 decreases the malignant phenotype of melanoma cells. (**a**) qRT–PCR analysis of TRIB2 mRNA levels in 361C and 361shTRIB cells. Error bars refer to standard error. Normalization of the results was performed by taking 18S mRNA levels as reference. (**b**) 361C and 361shTRIB cells were grown in standard culture conditions over a period of 10 days and cell density was measured every second day. The relative number of cells was estimated by crystal violet staining as described above. (**c**) In order to investigate their clonogenic potential, 361C and 361shTRIB cells were seeded at low density and allowed to grow for 10 days before fixation, crystal violet staining and quantification of the number of colonies formed. (**d**) 361C and 361shTRIB cells were seeded in soft agar and maintained for 1 month for anchorage-independent growth analysis. Bars refer to the average number of colonies obtained from triplicates of each cell line with their respective standard deviation. (**e**) Microscopic detail of the colonies formed by 361C and 361shTRIB cells in soft agar after 1 month of culture. (**f**) 361C and 361shTRIB cells were grown until confluence and their migratory capabilities were analyzed in a wound-healing assay.

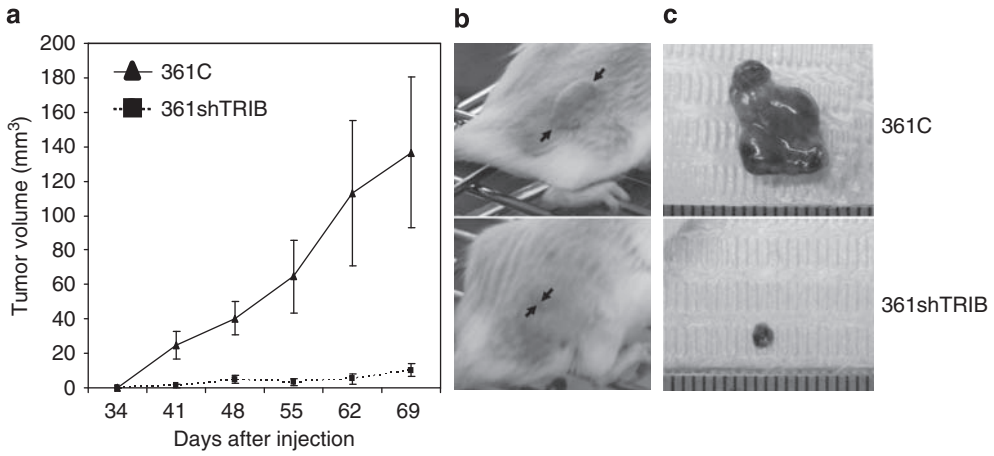

Figure 6 Silencing of TRIB2 reduces tumor growth *in vivo*. (**a**) 7×10^5 361shTRIB or 361C cells were xenografted in ZSCID mice and the growth of the tumors formed by each cell population was followed. The statistical significance for each time point was determined by unpaired *t*-test. Except for the time point at day 34, the comparison of the tumor volumes of the two mouse cohorts was statistically significant. The *P*-values for the time points at days 41–69 were 0.0075, 0.0024, 0.0082, 0.0149 and 0.0080, respectively. (**b**, **c**) At day 69, both groups of animals were photographed, euthanized, and tumors were dissected and photographed. Mice (**b**) and dissected tumors (**c**) representative for the both groups are depicted. The rulers at the bottoms of the photographs (**c**) are scaled in mm.

Discussion

The advent of RNAi-based functional genomics in mammals paved the way for unbiased screens in human cell systems. In the present work we report a large-scale loss of function screen aimed to identify and validate gene targets involved in the framework of signalling events that control the activity of FOXO transcription factors.

Based on two independent cell-based systems that were shown to effectively report FOXO-dependent transcriptional activity and subcellular localization of the GFP–FOXO fusion protein, we screened a vector-based RNAi expression library that directs the synthesis of shRNAs targeting for suppression 7914 different human genes. Those genes of which silencing produced positive hits in both screening systems were included in the high confidence list of FOXO suppressors. Among the selected genes were PIK3CA and Akt-3, components of the canonical PI3K/Akt pathway. Interestingly, silencing of the Ca^{2+}-binding protein Calmodulin 2 increased FOXO-driven luciferase activity and induced nuclear translocation of the GFP–FOXO reporter protein. These data are in agreement with the previous observation that inhibition of Calmodulin by its specific small-molecule inhibitors W7, W13 and Calmidazol led to the nuclear accumulation of FOXO (Zanella *et al*., 2008) and strengthens the notion that calcium signaling is an important factor influencing the subcellular localization of FOXO. The presence within our priority list of genes that are known to be involved in the regulation of FOXO validated the specificity of our screening systems. Among the genes that have not been previously associated with FOXO functions, we identified *TRIB2*, the human homolog of the *Drosophila* gene *tribbles*. *Tribbles* has been reported to regulate ventral furrow formation in *Drosophila* by binding to String or CDC25 (Grosshans and Wieschaus, 2000; Mata *et al*., 2000). The three human orthologs of *tribble*s, namely *TRIB1*, *TRIB2* and *TRIB3*, share a strong similarity in their amino-acid sequences, consisting essentially in their pseudokinase domain (Hegedus *et al*., 2006, 2007).

We found TRIB2 to be highly expressed specifically in melanoma malignancies, melanocyte-derived cells and melanoma cell lines. Interestingly, overexpression was not observed in samples from other tumor sources, including non-basal skin carcinoma. Our data suggest a potential use of TRIB2 as a diagnostic marker for the detection of malignant melanoma, although more studies are needed to confirm its utility as a tool in a diagnostic setting. Further experiments including a larger patient cohort with survival information must also elucidate its clinical significance.

The regulatory mechanisms that maintain high TRIB2 expression in melanocyte-derived cells remain unknown at present. TRIB2 expression might be regulated by lineage-specific signaling events such as the signal transduction cascade initiated by c-kit and shown to modulate the activity and stability of the tissue-restricted dimeric transcription factor MITF (Hou *et al*., 2000).

Malignant melanoma is one of the most aggressive human tumors that arise from the malignant transformation of melanocytes, the pigment-producing cells that reside in the basal epidermal layer of the human skin. Several signaling pathways are thought to exert key functions in melanoma development and progression, including Ras–Raf–MEK–ERK (MAPK) and the PI3K/Akt signaling pathways (Meier *et al*., 2007). A recent study reported the upregulation of miR-182 in melanoma cell lines and tissue samples promoting the repression of FOXO3a (Segura *et al*., 2009). Interestingly, ectopic expression of a non-phosphorylatable, constitutively nuclear form of FOXO has been shown to induce apoptosis in A375 melanoma cells (Hilmi *et al*., 2008).

In this study, we provide strong evidence for an alternative mode of FOXO inactivation in melanocyte-

derived and melanoma cells through overexpression of TRIB2. One appealing possibility is that downregulation of FOXO activity through TRIB2 is one of the elusive intrinsic survival features of paternal melanocytes that determines the aggressive and highly resistant behavior of melanocyte-derived malignancies nourished by additional alterations acquired during tumor progression (Soengas and Lowe, 2003).

In functional assays we could show that suppression of TRIB2 protein in melanoma cells resulted in a significant decrease in cell proliferation, cell migration and anchorage-independent growth. Thus, high TRIB2 expression could contribute to the formation and progression of melanoma lesions. Consistently, retroviral expression of *TRIB2* has been shown to immortalize hematopoietic progenitors and TRIB2-reconstituted mice uniformly developed fatal transplantable acute myelogenous leukemia (Keeshan *et al*., 2006). Our study further reveals that *in vivo* tumor formation of G-361 cells in immunocompromised mice was impaired upon silencing of *TRIB2*. Taken together, our data lead to the conclusion that TRIB2 can promote the growth of melanoma cells and support their *in vivo* tumorigenesis. Future experiments should determine whether TRIB2 is part of the differentiation program of normal melanocytes that predisposes their transformed derivatives to forming aggressive tumors (Gupta *et al*., 2005).

In summary, sophisticated cell-based screening systems allowed us to systematically interrogate the signaling network that controls the activity of FOXO proteins and to identify possible targets for the restoration of FOXO functions, independent of preconceived notions of mechanistic relationships. Our work identifies TRIB2 as a suppressor of FOXO activity overexpressed in malignant melanoma and provides evidence that TRIB2 contributes to the maintenance of the malignant phenotype of melanoma cells. Thus, further investigation into the role of TRIB2 in the pathogenesis of melanoma lesions may provide new therapeutic insights into this most aggressive form of skin cancer resistant to all standard anticancer therapies.

Materials and methods

Reagents and plasmids

LY294002 was purchased from Calbiochem (San Diego, CA, USA). Human insulin was purchased from Roche Diagnostics (Mannheim, Germany). The NKI shRNA libray was provided by R Bernards. The RNAi agents to validate TRIB2 silencing were purchased from Applied Biosystems (Foster City, CA, USA), Thermo Fisher Scientific (Waltham, MA, USA) and OriGene (Rockville, MD, USA). The sequences of the shRNAs and siRNAs are shown in Supplementary Table S2.

FOXO3a as well as a constitutively active construct, FOXO3a-(A)3, was kindly provided by Dr M Hu (University of Texas MD Anderson Cancer Center, Houston, TX, USA). FOXO1 and FOXO1-GFP were kindly provided by T Unterman (University of Illinois at Chicago, Chicago, IL, USA).

TRIB2 cDNA was amplified from HEK293T cells by PCR to be cloned into a pCDNA/V5/GW/D-TOPO vector. Subsequently, PCR was used to amplify TRIB2-V5 and the resulting fragment was cloned into a pIRESpuro2 vector. Mouse trb2 was a gift from E Kiss-Toth (University of Sheffield, Sheffield, UK).

Cell culture

All cell lines were obtained from the American Type Culture Collection. U2-OS, HEK293T, A375, Hs895T, Sk-Mel-94, Sk-Mel-19, UACC-257, Hs 895T, Sk-Mel-147, VA-13 and HaCaT cells were cultivated in Dulbecco's modified Eagle's medium (Sigma, St Louis, MO, USA), supplied with 10% fetal bovine serum (FBS). Sk-mel-5, Sk-mel-28, UACC62 and M14 cells were cultivated in RPMI supplemented with 10% FBS (Sigma). G-361 cells were maintained in Mc Coy's 5A medium complemented with 10% FBS. Previously described U2foxRELOC cells (Zanella *et al*., 2008) were cultivated in 10% FBS Dulbecco's modified Eagle's medium with 100 μg/ml G-418 (Gibco, Paisley, Scotland, UK). Human epidermal melanocytes were obtained from Cascade Biologics and maintained in medium 254 (Cascade Biologics, Portland, OR, USA) supplemented with HMGS (Cascade Biologics). Cell cultures were maintained in a humidified incubator at 37 °C with 5% CO_2.

Generation of 293foxREP cells

HEK293T cells were transfected with the plasmid pGL3-DBE3X-Luc-Puro (Zanella *et al*., 2009). Puromycin-resistant clones were assayed for luciferase activity and responsiveness to the inhibition of PI3K/Akt signaling. The most suitable clone was selected as the assay cell line and designated as 293foxREP.

Preparation of the shRNA library

Before its transfection the bacterial cultures of the arrayed shRNA library were replicated and purified. The replication was carried out using a Biomek FX liquid handler (Beckman-Coulter, Marseille, France). The plasmids contained in the bacterial cultures were purified using the Montage plasmid extraction kit of Millipore (Bedford, MA, USA) adapted to a vacuum manifold preceded by a preclearing with the Wizard SV96 lysate clearing plates of Promega (Madison, WI, USA).

Western blot analysis

Cells were lysed with 1 ml of a solution containing 50 mM Tris-Cl, 150 mM NaCl, 1% Igpal, 10 μg of aprotinin and 10 μg of leupeptin. After transference, nitrocellulose membranes were blocked in an infra-red specific solution (Li-Cor) for a minimum of 4 h, at 4 °C. Incubation with the primary antibodies was carried for 4–12 h, at 4 °C with constant shaking. TRIB2 levels were probed using an anti-V5 antibody (Invitrogen, Carlsbad, CA, USA) and α-tubulin levels were probed as a loading control with a commercially available antibody (Sigma). All dilutions used were as indicated in the manufacturers' instructions.

Luciferase assays

2×10^5 293foxREP cells were seeded per well in transparent round-bottom 96-well plates (Nunc, Roskilde, Denmark). Once attached, cells were co-transfected with 25 ng of the pCDNA3 vector containing cDNA for FOXO3a, 50 ng of the commercially available pRG-TK vector (Promega) containing *Renilla* luciferase cDNA for normalization of results and 25 ng of the empty pSuperRetro vector, pSuperRetro containing shRNAs against PI3K and Akt, or the shRNA pools contained in the library plate. All transfection experiments were performed in triplicate, with Effectene transfection reagent (Qiagen, Hilden, Germany) following the manufacturers' instructions. Automated luciferase assays were carried out using the Dual-Luciferase

Reporter Assay System (Promega), according to the manufacturer's instructions.

HCS assays
The workflow of the U2foxRELOC assay (Zanella *et al*., 2008), as well as the image and data analysis procedures, have been described previously (Zanella *et al*., 2007; Rosado *et al*., 2008).

Cancer-profiling array
PCR-amplified TRIB2 or ubiquitin cDNAs were radioactively labeled and hybridized subsequently to the Cancer Profiling Array II membrane (BD Biosciences, San Diego, CA, USA). The washed membrane was exposed to an Amersham Phosphor Screen overnight and scanned in a Typhoon-9400 Variable Mode Imager (Amersham Biosciences, Piscataway, NJ, USA). Quantification of the signals was carried in the Quantity One software version 4.5.2 (BioRad, München, Germany).

Quantitative RT–PCR
Total RNA was extracted using TRI-Reagent (Sigma), according to the manufacturers' indications. After RNA isolation, DNAse I (Roche) treatment was performed in the presence of an RNAse inhibitor (Roche, Mannheim, Germany). Purified RNAs were quantified in a NanoDrop 1000 spectrophotometer quality-checked in MOPS-1.2% agarose gel and cDNA synthesis was carried out using the High Capacity cDNA Reverse Transcription Kit (Applied Biosystems). PCR reactions were run in an ABI PRISM 7900HT sequence detection system (Applied Biosystems). Cycling conditions were set to 10 min at 95 °C, followed by 40 cycles of 15 s at 95 °C and 1 min at 60 °C. Identical PCR conditions were used with the human melanoma TissueScan Tissue Quantitative PCR Array (OriGene). Finally, a dissociation curve was plotted to check the specificity of amplification. Results were analyzed and the relative mRNA quantity calculated using the qBasePlus software (Hellemans *et al*., 2007).

Generation of 361C and 361shTRIB cells
G-361 cells were transfected using the Effectene (Qiagen) reagent, either with an empty pSuperRetro vector (361C) or with the validated TRIB2^{NKI} shRNA (361shTRIB). After selection with Puromycin, both cell populations were maintained in Mc Coy's 5A Medium supplemented with 10% FBS and 0.5 ug/ml puromycin.

Proliferation and doubling-time assay
At 24 h after seeding 361C and 361shTRIB cells, the growth medium was changed (day 0) and a point of the curve was taken every second day. Cells were fixed with 0.5% glutaraldehyde, stained with 1% crystal violet, lysed with 15% acetic acid and the lysis products were transferred to clear-bottom 96-well plates (Nunc). The absorbance at 590 nm wavelength was measured in a Victor3 (Perkin-Elmer, Foster City, CA, USA) plate reader.

Clonogenic assay
361C and 361shTRIB cells were seeded in triplicate at a density of 10^4 cells per well in 10-cm plates. The growth medium was changed every second day. At day 10 cells were fixed with 0.5% glutaraldehyde, stained with 1% crystal violet and the colonies were counted.

Growth in soft agar
The anchorage-independent growth of 361C and 361shTRIB cells was analyzed by seeding triplicates of 4×10^5 cells per well of each population in 1.4% agarose D-1 Low EEO (Pronadisa) growth medium containing 10% FBS, and disposed onto a previously solidified base of growth medium containing 2.8% agar (agarose D-1 Low EEO, Pronadisa, Madrid, Spain) in a six-well plate. Once the soft agar had been solidified, 1 ml of the growth medium was added. After 24 h, media containing 10% FBS was added to each well and renewed twice weekly. Colonies were scored after 1 month of growth. Photographs were taken in an Olympus CK40 microscope equipped with an Olympus DP12 camera (Olympus, Tokyo, Japan) at 40X magnification.

Wound-healing assays
361C and 361shTRIB cells were seeded in triplicate at a density of 5×10^5 cells per well in 24-well plates. Following attachment, a wound was produced in the cell monolayer, the growth medium was replaced and a picture was taken (day 0) in an Olympus CK40 microscope equipped with an Olympus DP12 camera at $\times 40$ magnification. Pictures were taken every 24 h in the same field.

Xenografts
ZSCID mice were injected with 7×10^5 361C and 361shTRIB cells and the growth of the resulting tumors was followed by direct measurement of tumour volume every 7 days over a total period of 69 days. The smallest and the largest diameter of tumors were measured with a digital caliper, and tumor volumes were calculated using the following formula: volume $(mm^3) = [(\text{smallest diameter})^2 \times (\text{largest diameter})]/2$. All values were presented as means ± s.e. The unpaired *t*-test (two-tailed) was performed for statistical analysis using the GraphPad PRISM Version 4.0 program.

Conflict of interest

The authors declare no conflict of interest.

Acknowledgements

This work was supported by a grant from the Spanish MEC (project BIO2006-02432). FZ is the recipient of a Marie Curie Fellowship. We acknowledge the expert technical assistance of D Megias, J C Cigudosa, J Monsech and O Dominguez. We thank M Hu, T Unterman and E Kiss-Toth for providing plasmids and JF Martinez for helpful discussions and critical reading of this paper. We are indebted to R Bernards for advice and for providing us with the NKI shRNA library.

References

Berns K, Hijmans EM, Mullenders J, Brummelkamp TR, Velds A, Heimerikx M *et al*. (2004). A large-scale RNAi screen in human cells identifies new components of the p53 pathway. *Nature* **428**: 431–437.

Birmingham A, Anderson EM, Reynolds A, Ilsley-Tyree D, Leake D, Fedorov Y *et al*. (2006). 3′ UTR seed matches, but not overall identity, are associated with RNAi off-targets. *Nat Methods* **3**: 199–204.

Brunet A, Bonni A, Zigmond MJ, Lin MZ, Juo P, Hu LS *et al*. (1999). Akt promotes cell survival by phosphorylating and inhibiting a Forkhead transcription factor. *Cell* **96**: 857–868.

Calnan DR, Brunet A. (2008). The FoxO code. *Oncogene* **27**: 2276–2288.

Dansen TB, Burgering BM. (2008). Unravelling the tumor-suppressive functions of FOXO proteins. *Trends Cell Biol* **18**: 421–429.

Gomes AR, Brosens JJ, Lam EW. (2008). Resist or die: FOXO transcription factors determine the cellular response to chemotherapy. *Cell Cycle* **7**: 3133–3136.

Grosshans J, Wieschaus E. (2000). A genetic link between morphogenesis and cell division during formation of the ventral furrow in Drosophila. *Cell* **101**: 523–531.

Gupta PB, Kuperwasser C, Brunet JP, Ramaswamy S, Kuo WL, Gray JW *et al*. (2005). The melanocyte differentiation program predisposes to metastasis after neoplastic transformation. *Nat Genet* **37**: 1047–1054.

Hegedus Z, Czibula A, Kiss-Toth E. (2006). Tribbles: novel regulators of cell function; evolutionary aspects. *Cell Mol Life Sci* **63**: 1632–1641.

Hegedus Z, Czibula A, Kiss-Toth E. (2007). Tribbles: a family of kinase-like proteins with potent signalling regulatory function. *Cell Signal* **19**: 238–250.

Hellemans J, Mortier G, De Paepe A, Speleman F, Vandesompele J. (2007). qBase relative quantification framework and software for management and automated analysis of real-time quantitative PCR data. *Genome Biol* **8**: R19.

Hilmi C, Larribere L, Deckert M, Rocchi S, Giuliano S, Bille K *et al*. (2008). Involvement of FKHRL1 in melanoma cell survival and death. *Pigment Cell Melanoma Res* **21**: 139–146.

Hou L, Panthier JJ, Arnheiter H. (2000). Signaling and transcriptional regulation in the neural crest-derived melanocyte lineage: interactions between KIT and MITF. *Development* **127**: 5379–5389.

Hu MC, Lee DF, Xia W, Golfman LS, Ou-Yang F, Yang JY *et al*. (2004). IkappaB kinase promotes tumorigenesis through inhibition of forkhead FOXO3a. *Cell* **117**: 225–237.

Huang H, Tindall DJ. (2007). Dynamic FoxO transcription factors. *J Cell Sci* **120**: 2479–2487.

Hui RC, Francis RE, Guest SK, Costa JR, Gomes AR, Myatt SS *et al* (2008). Doxorubicin activates FOXO3a to induce the expression of multidrug resistance gene ABCB1 (MDR1) in K562 leukemic cells. *Mol Cancer Ther* **7**: 670–678.

Keeshan K, He Y, Wouters BJ, Shestova O, Xu L, Sai H *et al* (2006). Tribbles homolog 2 inactivates C/EBPalpha and causes acute myelogenous leukemia. *Cancer Cell* **10**: 401–411.

Mata J, Curado S, Ephrussi A, Rorth P. (2000). Tribbles coordinates mitosis and morphogenesis in Drosophila by regulating string/CDC25 proteolysis. *Cell* **101**: 511–522.

Meier F, Busch S, Lasithiotakis K, Kulms D, Garbe C, Maczey E *et al* (2007). Combined targeting of MAPK and AKT signalling pathways is a promising strategy for melanoma treatment. *Br J Dermatol* **156**: 1204–1213.

Myatt SS, Lam EW. (2007). The emerging roles of forkhead box (Fox) proteins in cancer. *Nat Rev Cancer* **7**: 847–859.

Paik JH, Kollipara R, Chu G, Ji H, Xiao Y, Ding Z *et al* (2007). FoxOs are lineage-restricted redundant tumor suppressors and regulate endothelial cell homeostasis. *Cell* **128**: 309–323.

Rosado A, Zanella F, Garcia B, Carnero A, Link W. (2008). A dual-color fluorescence-based platform to identify selective inhibitors of Akt signaling. *PLoS ONE* **3**: e1823.

Segura MF, Hanniford D, Menendez S, Reavie L, Zou X, Alvarez-Diaz S *et al* (2009). Aberrant miR-182 expression promotes melanoma metastasis by repressing FOXO3 and microphthalmia-associated transcription factor. *Proc Natl Acad Sci USA* **106**: 1814–1819.

Soengas MS, Lowe SW. (2003). Apoptosis and melanoma chemoresistance. *Oncogene* **22**: 3138–3151.

Yang H, Zhao R, Yang HY, Lee MH. (2005). Constitutively active FOXO4 inhibits Akt activity, regulates p27 Kip1 stability, and suppresses HER2-mediated tumorigenicity. *Oncogene* **24**: 1924–1935.

Zanella F, Rosado A, Blanco F, Henderson BR, Carnero A, Link W. (2007). An HTS approach to screen for antagonists of the nuclear export machinery using high content cell-based assays. *Assay Drug Dev Technol* **5**: 333–341.

Zanella F, Rosado A, Garcia B, Carnero A, Link W. (2008). Chemical genetic analysis of FOXO nuclear-cytoplasmic shuttling by using image-based cell screening. *Chembiochem* **9**: 2229–2237.

Zanella F, Rosado A, Garcia B, Carnero A, Link W. (2009). Using multiplexed regulation of luciferase activity and GFP translocation to screen for FOXO modulators. *BMC Cell Biol* **10**: 14.

Supplementary Information accompanies the paper on the Oncogene website (http://www.nature.com/onc)